Effect of Local Molecular Shape and Anisotropic Reactivity on the Rate of Diffusion-Controlled Reactions

A. I. Shushin* and A. V. Barzykin†

*Institute of Chemical Physics, Russian Academy of Sciences, GSP-1, Moscow 117977, Russia, and †National Institute of Advanced Industrial Science and Technology, Tsukuba, Ibaraki 305-8565, Japan

ABSTRACT The role of distance-dependent anisotropic reactivity and molecular geometry in the vicinity of localized reaction centers in influencing the rate of bimolecular diffusion-controlled reactions is analyzed in detail, both analytically and numerically. The effect of local molecular shape is considered within the model of reflective hemispheres of small radius l_h on the surfaces of otherwise spherical molecules of radius R ($l_h \ll R$). The distance-dependent reactivity is modeled by reactive hemispheres of radius l_r on top of the reflective hemispheres ($l_r \ll R$). It is shown that the presence of the reflective hemispheres leads to a markedly large increase of the reaction rate. The maximum effect is $\sim R/l_h \gg 1$ times, as described by the ratio of local to average molecular curvature. It is observed for $l_h \approx R(l_r/R)^{1/2} \gg l_r$. The effect of thickness of the reaction regions is described within the model of reactive cylinders of height l_r and angular radius $\theta \ll 1$. It is shown that the characteristic parameter in the expansion of the reaction rate as a function of l_r/R is $l_r/(R\theta^2)$, and therefore, even for small relative thickness $d = l_r/\theta$, its effect on the rate is very strong, i.e., the conventional model of reactive patches, which assumes zero thickness of the reaction region, may considerably underestimate the reaction rate.

INTRODUCTION

The anisotropy of reactivity and interaction is an important property of molecules, especially those of large size: organic molecules, macromolecules, biomolecules, etc. It is known to strongly influence the kinetics of diffusion-controlled bimolecular reactions in liquids (McCammon, 1984). The effect of anisotropy is typically described in terms of the so-called steric factor f, which relates the observed reaction rate constant K to the one for isotropic molecules of the same size. The role of diffusion turns out to be rather nontrivial and manifests itself in a considerable enhancement of the reaction rate as compared to the rate estimated on the basis of simple geometrical arguments by taking f to be the ratio of the reactive part of the molecule to its full surface.

A number of different models have been formulated to describe the effect of anisotropy. The most popular one is the model of reactive patches (MRP) (Solc and Stockmayer, 1971, 1973; Schmitz and Schurr, 1972; Schurr and Schmitz, 1976; Shoup et al., 1981; Northrup et al., 1984; Temkin and Yakobson, 1984; Berg, 1985; Lee and Karplus, 1987; Zhou, 1993; Traytak, 1994, 1995; Zhou and Szabo, 1996a, 1996b), in which the reaction is assumed to occur whenever the circular reactive patches of zero thickness on the surfaces of the reacting molecules touch each other. The MRP, however, is not quite realistic, in a sense that it does not take into account the thickness of the reaction region, usually implied in any realistic (distance-dependent) mechanism of reactivity and interaction. More realistic in this sense is the model of reactive hemispheres (MRH), recently proposed and analyzed in detail by one of us (Shushin, 1986, 1988a,b, 1999, 2000). This model suggests the onset of the reaction upon overlapping of the hemispherical reaction regions whose centers, called the reactive centers (RCs), are located on the surfaces of molecules. The MRH was shown to predict the reaction rates much larger than those for the MRP with the same characteristic size of the reaction regions.

A detailed comparative study of the MRP and the MRH has been performed by using the method of local analysis, in the practically most interesting limit of strong anisotropy, where the size of the reaction region is much smaller than the size(s) of the molecule(s) (Shushin, 1986, 1988a,b, 1999, 2000; Barzykin and Shushin, 2001). The method is based on a simple observation that, in this limit, the reactive flux is determined by the specific features of relative motion of the molecules in the vicinity of reactive orientations, where the original curvilinear coordinates describing relative position of the pair of molecules can be approximated by the Cartesian ones. The study demonstrated a significant difference in the predictions of the MRP and the MRH for the reaction rate. It also revealed a strong dependence of both the MRP- and the MRH-reaction rates on the local (near RCs) specific features of molecular shape. Even relatively small deviation of the shape from spherical can lead to a fairly strong change in the reaction rate.

In this work, we investigate in detail the role of local molecular shape in the vicinity of the reaction region and the shape of the reaction region itself in influencing the rate of bimolecular diffusion-controlled reactions in the case where both reacting molecules are anisotropic. Both reactants are chosen to be anisotropic because the effects under study are expected to be most pronounced in this case (as compared to the case where only one molecule is anisotro-

Received for publication 14 May 2001 and in final form 20 August 2001.

Address reprint requests to A. V. Barzykin, National Institute of Advanced Industrial Science and Technology, Tsukuba Central 5, Tsukuba, Ibaraki 305-8565, Japan. Tel.: +81-298-61-9339; Fax: +81-298-61-4526; E-mail: a.barzykin@aist.go.jp.

0006-3495/01/12/3137/09 $2.00

pic). The problem is studied within the MRH both analytically (using the method of local analysis) and numerically (via Brownian dynamics simulations). To focus on the effects of molecular shape, we assume that there is no interaction potential. Nonspherical shape of the molecules near the RCs is modeled by reflective hemispheres of small radii (much smaller than the size of the molecules), with the RCs located on top of these hemispheres. This is a step toward real molecular geometry. The influence of the shape of the reaction regions (particularly, the thickness) is analyzed in the model of reactive cylinders (MRC), which is similar to the MRH but with hemispheres replaced by cylinders. Practically, this situation may be realized if a certain group of atoms served as the RCs. The height of the cylinder would then correspond to the reaction radius for one atom. Another example is electron transfer (through bonds) from a site buried within a molecule. On the basis of our analytical and numerical results, which have proven to be in quite a good agreement, we demonstrate that, first, local deviation of the molecular shape from the overall spherical can result in a significant change of the reaction rate and, second, even relatively small thickness of the reaction region can lead to a drastic acceleration of the reaction. Therefore, the MRP that assumes zero thickness of the reaction region may strongly underestimate the reaction rate.

THE MODEL OF REACTIVE HEMISPHERES

In this section, we present and briefly discuss the MRH as applied to spherical molecules, and consider the case where both reactants are anisotropic. The simpler case of one anisotropic molecule can be analyzed in a similar way. The general results obtained for spherical molecules will be used in our further discussion of the effect of nonsphericity.

The MRH, recently proposed and analyzed in detail (Shushin, 1986, 1988a,b, 1999, 2000) assumes that a molecule ν ($\nu = A, B$) is reactive within a certain distance l_{r_ν} from a point reactive center on its surface. The reaction occurs whenever the reactive hemispheres of two different molecules overlap or, equivalently, when the distance l between the reactive centers becomes smaller than $l_r = l_{r_A} + l_{r_B}$.

Here we consider the limit of strong anisotropy, where $l_{r_\nu} \ll R_\nu$ (R_ν denotes the radii of the molecules A and B), as the most interesting. Practically, one always has to deal with strong anisotropy of reactivity as far as large molecules are concerned (biomolecules, polymers, etc.). In this limit, the powerful method of local analysis can be applied. Because the details of the derivation have been thoroughly considered in a number of articles (Shushin, 1988a, 1999, 2000), here we restrict ourselves to an outline of the method and present only the final analytical expression for the case of two spherical molecules with anisotropic reactivity, which is to be compared with the new results.

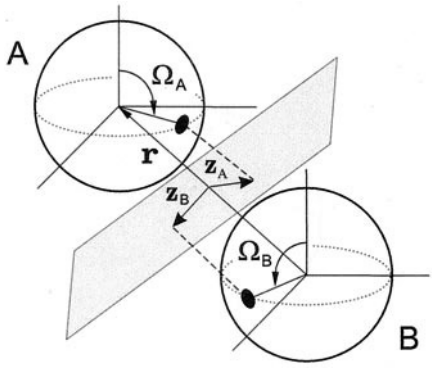

FIGURE 1 The coordinates describing relative orientation of the reaction centers on surfaces of molecules A and B.

In the method of local analysis, one considers relative diffusive motion of the molecules in close vicinity of the reactive orientations, where the system configuration can be represented as a point in five-dimensional space $\mathcal{M}_5$ of Cartesian coordinates. These coordinates are the normalized distance between the surfaces of the molecules, x_N, and the angular deviations of the reactive centers from the intermolecular axis $\mathbf{r}$, i.e., the normalized projection vectors $\mathbf{x}_\nu$ of the reactive centers onto the plane perpendicular to $\mathbf{r}$,

$$x_N = (r - R)/R; \quad \mathbf{x}_\nu = \mathbf{z}_\nu/R_\nu (\nu = A,B), \tag{1}$$

as shown in Fig. 1. Here $R = R_A + R_B$.

In the MRH, the shape of the reaction region S_r is determined by the condition that the distance l between the reactive centers is equal to the reaction radius, $l = l_r \equiv l_{r_A} + l_{r_B}$,

$$(\mu_A \mathbf{x}_A - \mu_B \mathbf{x}_B)^2 + (x_N + \tfrac{1}{2}\mu_A x_A^2 + \tfrac{1}{2}\mu_B x_B^2)^2 = \lambda_r^2, \tag{2}$$

where $\lambda_r = l_r/R$ and $\mu_\nu = R_\nu/R$. In the limit of strong anisotropy of reactivity ($\lambda_r \ll 1$), a convenient approximate expression for S_r can be obtained in coordinates

$$\mathbf{X}_1 = (\mu_A \mathbf{x}_A - \mu_B \mathbf{x}_B)/\Delta, \tag{3}$$

$$\mathbf{X}_2 = (\mu_B \mathbf{x}_A + \mu_A \mathbf{x}_B)/\Delta, \tag{4}$$

$$X_N = x_N, \tag{5}$$

where $\Delta = \sqrt{\mu_A^2 + \mu_B^2}$. We have

$$\Delta^2 X_1^2 + [X_N + (\tfrac{1}{2}\mu_A\mu_B/\Delta^2)X_2^2]^2 \approx \lambda_r^2. \tag{6}$$

Analysis of this expression shows that the shape of S_r is close to ellipsoidal with semiaxes

$$\lambda_1 = \lambda_r/\Delta, \quad \lambda_2 = \Delta\sqrt{2\lambda_r/(\mu_A\mu_B)}, \quad \text{and} \quad \lambda_N = \lambda_r. \tag{7}$$

The diffusion matrix in **X**-coordinates is nondiagonal with the following diagonal elements:

$$D_{11} = (\mu_A^2 D_{r_A} + \mu_B^2 D_{r_B} + D_N)/\Delta^2, \quad (8)$$

$$D_{22} = D_{11} + [(\mu_A - \mu_B)^2 - 1]D_N/\Delta^2, \quad (9)$$

$$D_{NN} = D_N = D/R^2, \quad (10)$$

where D is the relative translational and D_{r_ν} are the rotational diffusion coefficients. It can be rigorously shown that nondiagonal elements only weakly affect the absolute value of the reaction rate and thus can be neglected (Shushin, 2000). The limit of strong anisotropy corresponds to $\lambda_r \ll 1$, and thus $\lambda_2 \gg \lambda_1, \lambda_N$. Therefore, one can use the so-called adiabatic approximation and neglect the effect of diffusion along the coordinates $\mathbf{X}_2$, i.e., put $D_{22} = 0$ (Shushin, 1988a, 1999). By further assuming, for simplicity, that the reaction region S_r is spherical in the subspace $\{\mathbf{X}_1, X_N\}$ with the radius $\lambda = \lambda_r \approx \lambda_1$ (this approximation leads to a minor underestimation of the rate) one finally obtains for the steric factor (Shushin, 1988a, 1999, 2000).

$$f_0 = \frac{K}{4\pi DR} = \frac{\pi}{16}\left(\frac{l_r^2}{R_A R_B}\right)\frac{\sqrt{\delta(1+\delta)}}{\ln(\sqrt{1+\delta}+\sqrt{\delta})}, \quad (11)$$

where

$$\delta = (D_{r_A} R_A^2 + D_{r_B} R_B^2)/D. \quad (12)$$

Eq. 11 predicts the principally different dependence of the reaction rate on the size of the reactive sites than the MRP. In the MRP, one has $f \sim l_r^3$ for equal reactive sites, whereas $f \sim l_r^2$ in the MRH. Hence, the MRP rates are much smaller than the MRH rates for the same radii of the reactive regions. Comparison with the Brownian dynamics simulation results has demonstrated a very good accuracy of Eq. 11 even beyond the strict limit of strong anisotropy (Barzykin and Shushin, 2001).

THE MODELS OF NONSPHERICAL MOLECULAR SHAPE

The model of small reflective hemispheres

Assume that there are impenetrable hemispheres of radii l_ν ($\nu = A, B$) on the surfaces of otherwise spherical molecules and that the RCs are located on top of these hemispheres, as illustrated in Fig. 2. Simple estimation shows that, for small radii, $l_\nu < 0.4R_\nu$, the effect of these reflecting hemispheres on average geometric parameters of the molecules (i.e., average radii, etc.) is fairly small (about a few percent), and the anisotropy of rotational and translational diffusion coefficients can be neglected. In our further calculations, we will take the diffusion coefficients as equal to those for spherical molecules of radii R_ν. The model of reflecting hemispheres, however simplified it is, allows us to analyze the effect of local molecular geometry in the vicinity of the RCs on the diffusion-controlled reaction rate. The problem reduces to finding the shape of the reaction region S_r. It is impossible to determine S_r for any relation between l_ν and l_r, the reaction radius. Therefore, in what follows we will consider two limits: $l_\nu \gg l_r$ and $l_\nu \ll l_r$, and then bridge between these limits by a simple interpolation formula.

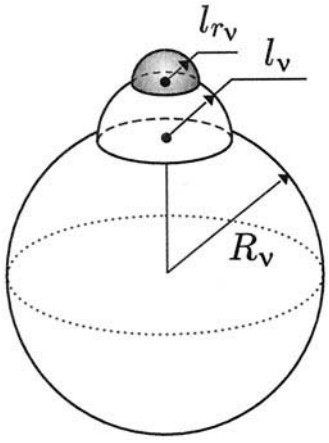

FIGURE 2 Schematic picture of the model of reflective hemispheres.

The case $l_\nu \gg l_r$

In the limit of relatively large reflective hemispheres, $l_\nu \gg l_r$ (but $l_\nu \ll R_\nu$), the reaction rate is determined by the local (small x_ν) shape of their contact surface S_h which can be written as (compare with Eq. 2)

$$(\mu_A \mathbf{x}_A - \mu_B \mathbf{x}_B)^2 + [x_N + \tfrac{1}{2}F_h(x_A, x_B)]^2 = \lambda_h^2, \quad (13)$$

where $\lambda_h = l_h/R \equiv (l_A + l_B)/R$ and

$$F_h(x_A, x_B) = \mu_A x_A^2 + \mu_B x_B^2. \quad (14)$$

The expression for the reaction region S_r will be similar to Eq. 2, but with the parameters corresponding to the centers of the reflecting hemispheres, μ_ν, R_ν, and R, replaced by those for the reaction centers, ξ_ν, L_ν, and L, i.e.,

$$\xi_\nu = L_\nu/L, \quad L_\nu = R_\nu + l_\nu, \quad \text{and} \quad L = L_A + L_B. \quad (15)$$

One should also take into account that, given a large curvature of the contact surface S_h (Eq. 13), the height $\tilde{x}_N = (r - L)/L$ of the reaction region S_r (i.e., the distance between the RCs along the axis **r**) is effectively decreased by

$$H(\mathbf{x}_A, \mathbf{x}_B) \approx \tfrac{1}{2}[F_h(x_A, x_B) + (\mu_A \mathbf{x}_A - \mu_B \mathbf{x}_B)^2/\lambda_h]. \quad (16)$$

Thus, the formula for the reaction region S_r can be written in the form

$$(\xi_A \mathbf{x}_A - \xi_B \mathbf{x}_B)^2 + [\tilde{x}_N - H(\mathbf{x}_A, \mathbf{x}_B) + \tfrac{1}{2} F_r(x_A, x_B)]^2 = \tilde{\lambda}_r^2, \tag{17}$$

where $\tilde{\lambda}_r = l_r/L = \lambda_r/(1 + \lambda_h)$ and

$$F_r(x_A, x_B) = \xi_A x_A^2 + \xi_B x_B^2. \tag{18}$$

Similar to the case of spherical molecules (see the preceding section), a convenient and quite accurate approximate expression for S_r in the limit of small $\tilde{\lambda}_r \ll \lambda_h$ can be obtained in coordinates

$$\mathbf{Z}_1 = (\xi_A \mathbf{x}_A - \xi_B \mathbf{x}_B)/\Delta_h \tag{19}$$

$$\mathbf{Z}_2 = (\xi_B \mathbf{x}_A + \xi_A \mathbf{x}_B)/\Delta_h, \tag{20}$$

$$Z_N = \tilde{x}_N, \tag{21}$$

where $\Delta_h = \sqrt{\xi_A^2 + \xi_B^2}$. The result is

$$Z_1^2 + [Z_N + (\tfrac{1}{2} \xi_A \xi_B/\Delta_h^2)\Phi Z_2^2]^2 \approx \tilde{\lambda}_r^2, \tag{22}$$

with

$$\Phi = (l_A l_B)/(R^2 \lambda_h \xi_A \xi_B). \tag{23}$$

Calculation similar to that leading to Eq. 11 gives for the steric factor,

$$f_h = \frac{K}{4\pi DL} = \frac{\pi}{16}\lambda_h \left(\frac{l_r^2}{l_A l_B}\right) \frac{\sqrt{\delta_h(1 + \delta_h)}}{\ln(\sqrt{1 + \delta_h} + \sqrt{\delta_h})}, \tag{24}$$

where

$$\delta_h = (D_{r_A} L_A^2 + D_{r_B} L_B^2)/D. \tag{25}$$

Taking into account that, in the considered limit of $l_\nu \ll R_\nu$, one can take $\delta_h \approx \delta$, the steric factor f_h can be conveniently represented in the simple form,

$$\frac{f_h}{f_0} = \kappa_> \approx \frac{\lambda_h}{\lambda_A \lambda_B} = \frac{l_A^{-1} + l_B^{-1}}{R_A^{-1} + R_B^{-1}}, \tag{26}$$

where f_0 is the steric factor for spherical molecules (without reflective hemispheres, see Eq. 11) and $\lambda_\nu = l_\nu/R_\nu$. Formula 26 shows that for $l_\nu \sim l \ll R_\nu \sim R$ the rate constant is determined by the local curvature radii in the vicinity of the RCs and thus it is increased by a factor of $f_h/f_0 \sim R/l \gg 1$ due to the presence of the reflective hemispheres, in agreement with general predictions (Shushin, 1999, 2000).

The case $l_\nu \ll l_r$

For small radii of the reflective hemispheres, $\zeta = l_h/l_r \ll 1$, their shape is of no consequence, because the reactive hemispheres will overlap before the reflective hemispheres can make contact. What matters is that the position of the RCs with respect to the spherical surface of the molecules is effectively raised by l_ν. The size $x_N = (r - R)/R$ of the reaction surface S_r along the axis $\mathbf{r}$ is, therefore, increased by $l_h = l_A + l_B$, so that the shape of S_r is determined as

$$X_1^2 + [X_N - \lambda_h + (\tfrac{1}{2} \mu_A \mu_B/\Delta^2) X_2^2]^2 \approx \lambda_r^2, \tag{27}$$

where X_j are defined in Eqs. 3–5. As a result, the height h_r of the reaction region and the characteristic size Λ_2 in the subspace $\{\mathbf{X}_2\}$ are also increased,

$$h_r = h_r^0(1 + \zeta) \tag{28}$$

$$\Lambda_2 = \Lambda_2^0 \sqrt{1 + \zeta}, \tag{29}$$

where $h_r^0 = \lambda_r$ and $\Lambda_2^0 = \Delta\sqrt{2\lambda_r/(\mu_A \mu_B)}$ are the corresponding parameters in the absence of the reflective hemispheres.

We recall that in the MRP, S_r is of an ellipsoid-like shape with small dimensions $\sim l_r$ in the 3D subspace $\{\mathbf{X}_1, X_N\}$ and large dimensions $\Lambda_2 \sim \sqrt{R l_r} \gg l_r$ in the 2D subspace $\{\mathbf{X}_2\}$. According to the predictions of the adiabatic approximation applied in this limit (Shushin, 1988a, 1999, 2000), the reaction rate constant K is given by the rate in the 3D-subspace, $K_3 \sim l_r$, integrated over the area of S_r in the 2D-subspace, $\sim \Lambda_2^2$, i.e., $K \sim K_3 \Lambda_2^2$. The increase of the height h_r results in the approximately spheroidal shape of S_r in the 3D subspace. This spheroidal distortion leads to the following change of the reaction rate in this subspace:

$$\frac{K_3}{K_3^0} = \frac{\sqrt{(1 + \zeta)^2 - 1}}{\ln[(1 + \zeta) + \sqrt{(1 + \zeta)^2 - 1}]} \approx 1 + \zeta, \tag{30}$$

where K_3^0 is the rate in the absence of the reflective hemispheres. Taking Eq. 29 into account, we finally obtain

$$f_h/f_0 = \kappa_< \approx (1 + \zeta)^2 \approx 1 + 2\zeta. \tag{31}$$

The case $l_\nu \sim l_r$

The limiting formulas 26 and 31 predict two opposite tendencies in the behavior of the steric factor as a function of ζ. Therefore, there should be an extremum. One can combine Eqs. 26 and 31 into a standard interpolation type of expression

$$\kappa = 1/(\kappa_<^{-n} + \kappa_>^{-n})^{1/n}, \tag{32}$$

which is expected to give reasonable accuracy for any relation between l_ν and l_r. The optimal value of the power n can be chosen by comparing Eq. 32 with numerical results. As n increases, the maximum of $\kappa(\zeta)$ becomes more sharp

and ultimately assumes an edge-like shape in the limit of $n \to \infty$. However, semiquantitative estimation of the value of $\kappa = f_h/f_0$ at the maximum (i.e., the maximum effect of the reflective hemispheres), can be made without the interpolation formula 32. To demonstrate the main features of the function $\kappa(\zeta)$, let us consider the case of identical molecules: $R_A = R_B = R/2$, $l_A = l_B = l_h/2$. The maximum $\kappa = \kappa_m$ is observed at $\lambda_h = \lambda_m$ for which $\kappa_< = \kappa_>$, i.e., $1 + 2\lambda_m/\lambda_r = 1/\lambda_m$. This relation yields $\lambda_m = 2/(1 + \sqrt{1 + 8/\lambda_r})$ and thus $\kappa_m = 1/\lambda_m = \frac{1}{2}(1 + \sqrt{1 + 8/\lambda_r})$. In the considered limit of $\lambda_r \ll 1$, the maximum value is given by $\kappa_m \approx \sqrt{2/\lambda_r} \gg 1$.

Numerical results

To test the conclusions of our analytical analysis, we have performed Brownian dynamics simulations using a method described in detail elsewhere (Barzykin and Shushin, 2001). Briefly, the method takes advantage of the exact asymptotic formula for the long-time behavior of the pair survival probability $S(t)$ (Shushin, 1988a, 1999),

$$S(t) = S(\infty)\left[1 + \frac{K}{4\pi D}(\pi D t)^{1/2}\right], \qquad (33)$$

that is valid for $t \gg R^2/D$ for any model of anisotropic reactivity, any shape of molecules, and any model of relative diffusion (except for the case where rotations of both molecules are frozen). The parameter $S(\infty)$ defines the total escape probability and depends on the initial condition. Numerically, we initiated the trajectories near the reaction region and then moved the molecules using standard Brownian dynamics algorithms (Ermak and McCammon, 1978; Kim and Lee, 1990). The trajectories were terminated either when the reaction criteria were satisfied (when the reaction hemispheres overlapped) or when a sufficiently large cutoff time was exceeded. After a sufficiently large number of trajectories were run, the asymptotic decay kinetics of the resulting average survival probability was fit to Eq. 33.

For illustration, we consider identical molecules with $R_A = R_B = R/2$ and $l_A = l_B = l_h/2$, and assume that friction is of Stokes type, i.e., $D_{r_A}R_A^2/D = D_{r_B}R_B^2/D = 0.375$. We do not have to specify the reaction radii for each molecule because, in the MRH, the reactivity depends only on l_r. Figure 3 presents the simulation results for the steric factor as a function of the normalized reaction radius on a log–log plot for different radii of the reflective hemispheres. All the predicted tendencies are clearly observed, namely: the reaction rate in the presence of the reflective hemispheres is considerably larger than that for spherical molecules, and the rate decreases as the radii of the reflective hemispheres are increased for small l_r and vice versa for large l_r. Figure 4 demonstrates that there is indeed a maximum in the reaction rate as a function of l_h. The limiting expressions 26 and 31 prove to be sufficiently accurate, and Eq. 32 with $n = 2$ provides a reasonable interpolation. Simple analytical estimations of the position of the maximum and the value of the maximum steric factor, as discussed in the preceding section, are in good agreement with simulations: we obtain $\lambda_m \approx 0.14$, $f_m \approx 0.014$ for $\lambda_r = 0.04$ and $\lambda_m \approx 0.22$, $f_m \approx 0.052$ for $\lambda_r = 0.1$ (see Fig. 4 for comparison).

As one can see, the effect of nonsphericity can be quite significant, in accord with earlier predictions (Shushin,

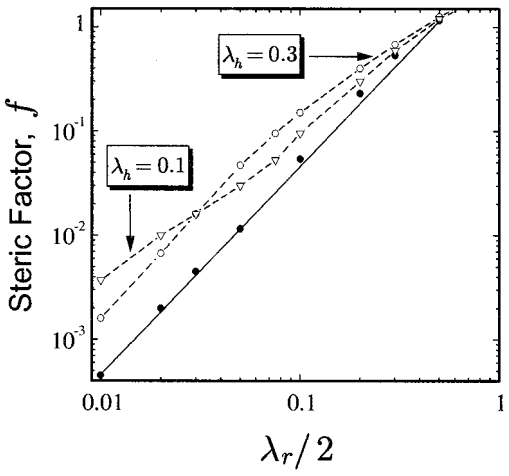

FIGURE 3 A plot of the Brownian dynamics simulation results for the effective steric factor f as a function of the relative reaction radius λ_r for two identical anisotropically reactive molecules with $D_{r_A}R_A^2/D = D_{r_B}R_B^2/D = 0.375$. Solid circles correspond to the MRH, and open symbols to the model of reflective hemispheres, as explained in the text. The solid line represents Eq. 11.

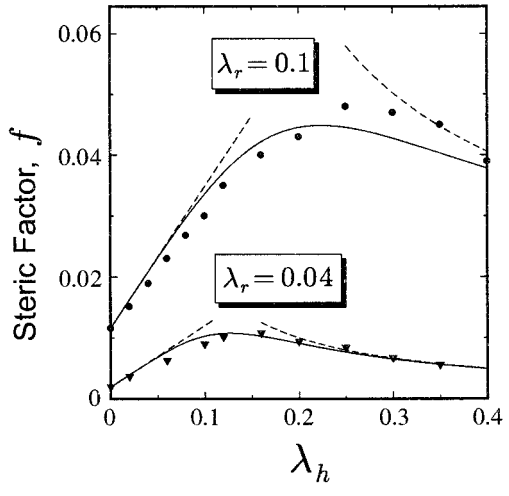

FIGURE 4 A plot of the Brownian dynamics simulation results (*symbols*) for the effective steric factor f within the model of reflective hemispheres for the case of two identical anisotropically reactive molecules with $D_{r_A}R_A^2/D = D_{r_B}R_B^2/D = 0.375$. Dashed lines represent the limiting solutions, Eqs. 26 and 31. Solid lines show the interpolation formula 32 with $n = 2$.

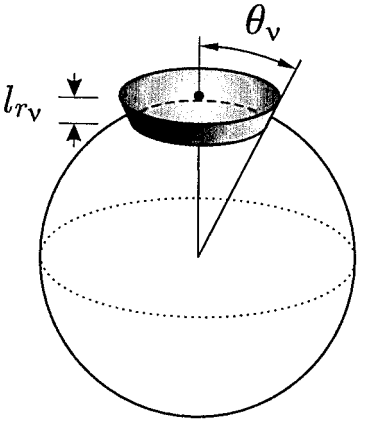

FIGURE 5 Schematic picture of the model of reactive cylinders.

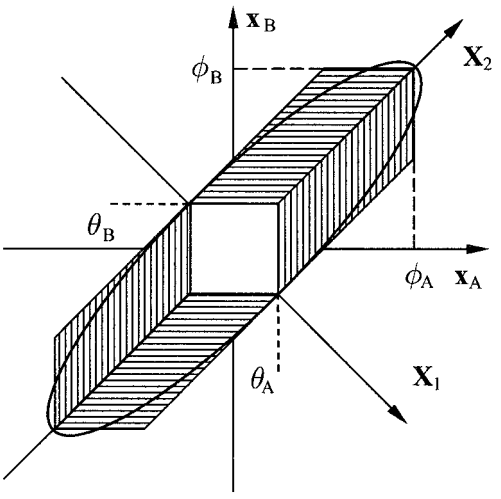

FIGURE 6 Projection of the reaction region into the subspace $\{\mathbf{x}_A, \mathbf{x}_B\}$ for the case of identical molecules. Here $\phi_A = \phi_B = \Lambda_2/\sqrt{2}$. See Appendix.

1999, 2000). It is local molecular geometry in the vicinity of the RCs that plays a crucial role in this effect.

The model of reactive cylinders

The conventional MRP can be regarded as the limit where a group of atoms or molecular fragments function as the RCs and the characteristic size of this group is much larger than the reaction radius for an individual atom. In other words, the thickness of the reaction region is negligibly small. We have seen, for the case of one RC, that the distance-dependent nature of reactive interactions, which is at the heart of the MRH, leads to a profound increase of the diffusion-controlled reaction rate (Shushin, 1986, 1988a,b, 1999, 2000; Barzykin and Shushin, 2001). Therefore, it is not obvious whether this effect can indeed be neglected even if there are many RCs.

To illustrate the effect of thickness of the reaction region, we introduce the MRC, i.e., the reactive sites on the surfaces of molecules are assumed to have conic shape with circular bases of angular radii θ_ν and heights l_{r_ν} ($\nu = A, B$), as shown in Fig. 5. Strictly speaking, these regions are not actually cylinders, but, in the considered limit of strong anisotropy of reactivity (i.e., small angular sizes, $\theta_\nu \ll 1$), the difference of the shape from cylindrical is negligibly small. It is clear that, for $l_{r_\nu} = 0$, the MRC reduces to the conventional MRP.

The shape of the reaction region S_r in the 5D-space $\mathcal{M}_5\{\mathbf{x}_A, \mathbf{x}_B, x_N\}$ corresponding to this simple model is fairly complicated. However, as discussed in the Appendix, it is relatively smooth and can be approximated by a semi-ellipsoid ($x_N \le 0$) shown in Fig. 6, which reduces to the circumscribed one for $l_{r_\nu} = 0$ (i.e., in the limit of reactive patches). In general, the expressions for the angles of orientation of this semi-ellipsoid and its semi-axes lengths are cumbersome. For illustration of the specific features of the reaction rate dependence on the thickness of the reaction regions, it is sufficient to consider the case of identical molecules: $R_A = R_B = R/2$, $\theta_A = \theta_B = \theta$, $l_{r_A} = l_{r_B} = l_r/2$, and $D_{r_A} = D_{r_B} = D_r$. Approximate ellipsoidal shape of S_r can then be represented as

$$(X_N/\lambda)^2 + (X_1/\Lambda_1)^2 + (X_2/\Lambda_2)^2 = 1, \qquad (34)$$

where

$$\lambda_r = l_r/R, \quad \Lambda_1 = \sqrt[4]{2}\theta, \quad \Lambda_2 = \sqrt[4]{2}\theta + \sqrt{2}\varphi, \qquad (35)$$

and $\varphi = \arccos[R/(R + l_r)] \approx \sqrt{2\lambda_r}$. Here we used an effective value of the angular radius, $\theta_{eff} = \theta/\sqrt[4]{2}$, which is given by the geometric mean of the radii of circumscribed and inscribed circles. Such an approximation is justified for $l_r < \theta$. Diagonal elements of the diffusion matrix in ($\mathbf{X}_1$, $\mathbf{X}_2$, X_N)-coordinates are given by

$$D_{11} \approx \tfrac{1}{2}D_r + D_N, \quad D_{22} = D_r, \quad \text{and} \quad D_N = D/R^2. \qquad (36)$$

Nondiagonal elements of this matrix do not affect the reaction and can be neglected, as before.

Using Eqs. 34–36 and the expressions derived earlier (Shushin, 1988a), one can calculate the reaction rate K_5 in the 5D-space $\mathcal{M}_5\{\mathbf{X}_1, \mathbf{X}_2, X_N\}$,

$$K_5 = (8\pi/3)(D_{11}D_{22}/D_N)\Delta^{-1}, \qquad (37)$$

where

$$\Delta = \int_0^\infty \frac{dx}{(x + a_1^2)(x + a_2^2)\sqrt{x + \lambda_r^2}}$$

$$= 2\,\frac{v_1 \arctan v_2 - v_2 \arctan v_1}{(a_1^2 - a_2^2)v_1 v_2 \lambda_r} \qquad (38)$$

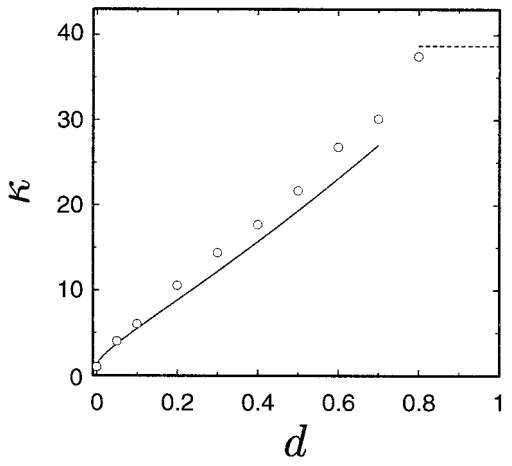

FIGURE 7 Brownian dynamics simulation results (*open circles*) for the relative steric factor as a function of relative thickness of the reaction region within the model of reactive cylinders for the case of two identical anisotropically reactive molecules with $D_{r_A}R_A^2/D = D_{r_B}R_B^2/D = 0.375$. Solid line represents Eq. 40. Dashed line corresponds to the steric factor for the MRH with the reaction radius equal to the radius of the cylinder base.

with

$$a_j = \Lambda_j \sqrt{D_N/D_{jj}},$$

$$v_j = \sqrt{(a_j/\lambda_r)^2 - 1}. \tag{39}$$

The observed reaction rate K is proportional to K_5, and so is the steric factor f_c. We finally obtain,

$$\kappa = f_c/f_0 = \frac{\pi}{2}\left(\frac{a_1^2 - a_2^2}{a_{10} + a_{20}}\right)\frac{\lambda_r v_1 v_2/(a_{10}a_{20})}{v_1 \arctan v_2 - v_2 \arctan v_1}, \tag{40}$$

where f_0 refers to the MRP for patches of angular radii θ, and $a_{j0} = a_j(l_r = 0) = \sqrt[4]{2}\,\theta\,(D_N/D_{jj})^{1/2}$. Eq. 40 is our main result for the MRC.

Numerical results

As for the model of reflective hemispheres, we consider the reaction between identical molecules and assume that friction is of Stokes type, i.e., $D_{r_A}R_A^2/D = D_{r_B}R_B^2/D = 0.375$. We fix the base radii θ of the reactive quasicylinders and vary their height. The simulation scheme is the same. Figure 7 shows that the reaction rate increases rapidly as the thickness of the reaction regions is increased. For the parameters chosen ($\theta \simeq 0.1$), the MRC rate becomes an order of magnitude larger than the MRP rate already for fairly small relative values of the cylinder height, $d = \lambda_r/\theta \sim 0.2$. The steric factor for the MRC with the height equal to the radius of the base ($d \simeq 1$) should be similar to (a little larger than) that for the MRH. This is indeed what we observe in simulations.

Theoretical estimations are in good agreement with the simulation results. The rate is somewhat underestimated and the discrepancy grows with l_r. This is understandable because, as l_r is increased, the shape of the reaction regions deviates more and more from cylindrical. Despite the fact that the MRC should rather be considered as a semiquantitative model, Eq. 40 is expected to reproduce the dependence of the reaction rate on the reaction region thickness quite accurately. Simple analysis of Eq. 40 shows that, if we try to expand f_c in power series of λ_r, the relevant parameter that will appear is $\sqrt{\lambda_r}/\theta = \sqrt{d/\theta}$ (at least for the first two terms). Because θ itself is a small parameter, the rate will increase rapidly with d.

CONCLUDING REMARKS

We have analyzed in detail the role of distance-dependent anisotropic reactivity and molecular geometry in the vicinity of localized reaction centers in influencing the rate of bimolecular diffusion-controlled reactions.

We have shown that local molecular shape is of critical significance. High local curvature may lead to a markedly large increase of the reaction rate with respect to that calculated using average molecular parameters. We have already demonstrated in our previous works (Shushin, 1999, 2000; Barzykin and Shushin, 2001) that the conventional MRP considerably underestimates the reaction rate if the RCs are strongly localized (point RCs). For example, the rate predicted by the MRP is about 50 times larger than the MRH rate for the same angular size of the reaction regions, $\theta = 0.1$. The neglect of the local nonspherical shape of molecules may lead, according to our results, to an additional underestimation of the rate of about 3–4 times, so that, in total, the error of the conventional MRP can be as large as about 200 times(!) and even larger for smaller relative size of the reaction regions.

We have confirmed that, in the limit of strong anisotropy of reactivity, the thickness of the reaction regions is also of crucial importance and leads to a considerable acceleration of the reaction even when it is much smaller than the angular size. The conventional model of reactive patches, which assumes zero thickness of the reaction region, may thus strongly underestimate the rate even if the RCs are not localized. For example, a relatively small thickness, five times smaller than the angular size θ, results in as much as an order of magnitude increase of the reaction rate for $\theta = 0.1$, with respect to the rate predicted by the MRP. Similar effects have been discussed within the model of buried point RCs (Shushin, 2000). We may conclude that, in general, the distance-dependent nature of reactive interactions is responsible for a significant rate enhancement as compared to contact diffusion-controlled reaction models, particularly in the limit of strong anisotropy of reactivity.

Note that $\theta = 0.1$ is quite a typical value for proteins. For example, $\theta = 3^\circ \simeq 0.05$ is quoted for barnase and bastar

(Vijayakumar et al., 1998), $\theta = 5^\circ \simeq 0.09$ for ferricytochrome c and ferrocytochrome b_5 (Eltis et al., 1991). Association rate contants up to $\sim 5 \times 10^9\ M^{-1}\ s^{-1}$ have been measured for these (Eltis et al., 1991; Schreiber and Fersht, 1993, 1996) and many other protein complexes (Wallis et al., 1995; Wendt et al., 1997), which is as much as four orders of magnitude larger than is expected from the MRP. Such incredibly high values have been attributed mainly to favorable electrostatic interactions between the associated proteins, as revealed by an experimentally observed (Eltis et al., 1991; Schreiber and Fersht, 1993, 1996; Wallis et al., 1995; Wendt et al., 1997) and theoretically confirmed (Eltis et al., 1991; Schreiber and Fersht, 1996; Gabdoulline and Wade, 1997; Vijayakumar et al., 1998) considerable decrease in the association rate constant with increasing ionic strength of the solution. However, additional effects can be due to long-range reactive interactions and local molecular shape, as discussed in this paper. For example, the hard-sphere radius of cytochrome c is 16.6 Å and thus the radius of the reactive patch on its surface is approximately 16.6 Å $\times$ 0.09 $\simeq$ 1.5 Å, which is not much larger than a typical electron transfer distance of 0.83 Å for these types of systems (Eltis et al., 1991) and comparable to a typical atomic radius. Given these parameters, we may expect two orders of magnitude increase in the association rate constant over the predictions of the MRP model solely due to the long-range nature of reactive interactions (electron transfer in this case) and the effect of local molecular shape. Detailed comparison of the relative contribution of electrostatic and reactive interactions to the overall enhancement of the protein–protein association rate requires a separate study, which is currently underway.

APPENDIX: THE SHAPE OF S_r IN THE MRC

The shape of the reaction region S_r in the 5D-space $\mathcal{M}_5\{\mathbf{x}_A, \mathbf{x}_B, x_N\}$ corresponding to the relatively simple model of reactive cylinders is fairly complicated. Its projection into the space $\{\mathbf{x}_A, \mathbf{x}_B\}$ is schematically shown in Fig. 6 for the case of identical molecules. Some additional ideas on the shape of S_r can be gained by taking into account that, at small $x_\nu < \theta_\nu$, i.e., for $x_N = l_r$, it coincides with that for conventional reactive patches (of zero height). Recall that, in the MRP, S_r in $\mathcal{M}_5$ is a 5D-cylinder with circular shape in the subspaces $\{\mathbf{x}_\nu\}$. Its projection into the space $\{\mathbf{x}_A, \mathbf{x}_B\}$ is a rectangle (unshaded rectangle at the origin in Fig. 6). It should also be noted that, for relatively large $x_\nu > \theta_\nu$, the region S_r can be qualitatively thought of as a figure created by displacing the above-mentioned MRP region along the coordinate X_2 with the height monotonically decreasing with increasing X_2: $\tilde{l}_r(X_2) \approx l_r - (\frac{1}{2}\,\mu_A\mu_B/\Delta^2)X_2^2$ (see Eq. 6). This fact can be understood as follows. By definition, the coordinate X_2 determines the position of patches by each other (for $X_1 = 0$), when the vector of relative position of the patch centers is parallel to the axis $\mathbf{r}$. The central points of the upper bases of cylinders lose contact just for $\tilde{l}_r + (\frac{1}{2}\,\mu_A\mu_B/\Delta^2)X_2^2 = l_r$. The shade lines parallel to $\mathbf{x}_A$ and $\mathbf{x}_B$ in Fig. 6 indicate that the corresponding cross-section of S_r is similar to that for the MRP-region located near the origin (i.e., at $\mathbf{x}_A = \mathbf{x}_B = 0$). The same can be said about the shape of S_r near the edges where $l_r = 0$.

The main goal of this fairly detailed discussion of the shape was to demonstrate that the reaction region S_r is relatively smooth. This is the only thing we need to know about the shape in addition to the sizes of S_r along different axes, because, in reality, it is impossible to solve the diffusion equation with the absorption boundary condition on S_r of this shape. This is why, for semiquantitative description, we approximate S_r by a semi-ellipsoid ($x_N \leq 0$) shown in Fig. 6, which reduces to the circumscribed one for $l_r = 0$ (i.e., in the limit of reactive patches).

REFERENCES

Barzykin, A. V., and A. I. Shushin. 2001. Effect of anisotropic reactivity on the rate of diffusion-controlled reactions. Comparative analysis of the models of patches and hemispheres. *Biophys. J.* 80:2062–2073.

Berg, O. G. 1985. Orientation constraints in diffusion-limited macromolecular association. The role of surface diffusion as a rate-enhancing mechanism. *Biophys. J.* 47:1–14.

Eltis, L. D., R. G. Herbert, P. D. Barker, A. G. Mauk, and S. H. Northrup. 1991. Reduction of horse heart ferricytochrome *c* by bovine liver ferrocytochrome b_5. Experimental and theoretical analysis. *Biochemistry.* 30:3663–3674.

Ermak, D. L., and J. A. McCammon. 1978. Brownian dynamics with hydrodynamic interactions. *J. Chem. Phys.* 69:1352–1360.

Gabdoulline, R. R., and R. C. Wade. 1997. Simulation of the diffusional association of barnase and bastar. *Biophys. J.* 72:1917–1929.

Kim, D., and S. Lee. 1990. A Brownian dynamics method for systems of nonspherical Brownian particles. *Bull. Korean Chem. Soc.* 11:127–131.

Lee, S., and M. Karplus. 1987. Kinetics of diffusion-influenced bimolecular reactions in solution. II. Effect of the gating mode and orientation-dependent reactivity. *J. Chem. Phys.* 86:1904–1921.

McCammon, J. A. 1984. Protein dynamics. *Rep. Progr. Phys.* 47:1–46.

Northrup, S. H., S. A. Allison, and J. A. McCammon. 1984. Brownian dynamics simulation of diffusion-influenced bimolecular reactions. *J. Chem. Phys.* 80:1517–1524.

Schmitz, K. S., and J. M. Schurr. 1972. The role of orientation constraints and rotational diffusion in bimolecular solution kinetics. *J. Phys. Chem.* 76:534–545.

Schreiber, G., and A. R. Fersht. 1993. Interaction of barnase with its polypeptide inhibitor barstar studied by protein engineering. *Biochemistry.* 32:5145–5150.

Schreiber, G., and A. R. Fersht. 1996. Rapid, electrostatically assisted association of proteins. *Nature Struct. Biol.* 3:427–431.

Schurr, J. M., and K. S. Schmitz. 1976. Orientation constraints and rotational diffusion in bimolecular solution kinetics. A simplification. *J. Phys. Chem.* 80:1934–1936.

Shoup, D., G. Lipari, and A. Szabo. 1981. Diffusion-controlled bimolecular reaction rates. The effect of rotational diffusion and orientation constraints. *Biophys. J.* 36:697–714.

Shushin, A. I. 1986. Recombination kinetics of molecules with anisotropic reactivity and interaction potential. Exact solution for a small reactive region. *Chem. Phys. Lett.* 130:452–457.

Shushin, A. I. 1988a. Diffusion controlled reaction rate of molecules with anisotropic reactivity and interaction potential. *Chem. Phys.* 120: 91–102.

Shushin, A. I. 1988b. Magnetic field effects in reactions of geminate recombination of anisotropic radicals. *Mol. Phys.* 64:65–80.

Shushin, A. I. 1999. Manifestation of anisotropic reactivity and molecular interactions in chemical reaction kinetics. *J. Chem. Phys.* 110: 12044–12058.

Shushin, A. I. 2000. The effect of anisotropic reactivity and interaction potential on the kinetics of diffusion controlled reactions. *J. Chem. Phys.* 113:4305–4314.

Solc, K., and W. H. Stockmayer. 1971. Kinetics of diffusion-controlled reaction between chemically asymmetric molecules. I. General theory. *J. Chem. Phys.* 54:2981–2988.

Solc, K., and W. H. Stockmayer. 1973. Kinetics of diffusion-controlled reaction between chemically asymmetric molecules. II. Approximate steady-state solution. *Int. J. Chem. Kinet.* 5:733–752.

Temkin, S. I., and B. I. Yakobson. 1984. Diffusion-controlled reactions of chemically anisotropic molecules. *J. Phys. Chem.* 88:2679–2682.

Traytak, S. D. 1994. The steric factor in the time-dependent diffusion-controlled reactions. *J. Phys. Chem.* 98:7419–7421.

Traytak, S. D. 1995. Diffusion-controlled reaction rate to an active site. *Chem. Phys.* 192:1–7.

Vijayakumar, M., K.-Y. Wong, G. Schreiber, A. R. Fersht, A. Szabo, and H.-X. Zhou. 1998. Electrostatic enhancement of diffusion-controlled protein–protein association: comparison of theory and experiment on barnase and bastar. *J. Mol. Biol.* 278:1015–1024.

Wallis, R., G. R. Moore, R. James, and C. Kleanthous. 1995. Protein–protein interactions in colicin E9 DNase-immunity protein complexes. 1. Diffusion-controlled association and femtomolar binding for the cognate complex. *Biochemistry.* 34:13743–13750.

Wendt, H., L. Leder, H. Härmä, I. Jelesarov, A. Baici, and H. R. Bosshard. 1997. Very rapid, ionic strength-dependent association and folding of a heterodimeric leucine zipper. *Biochemistry.* 36:204–213.

Zhou, H.-X. 1993. Brownian dynamics study of the influences of electrostatic interactions and diffusion on protein–protein association kinetics. *Biophys. J.* 64:1711–1726.

Zhou, H.-X., and A. Szabo. 1996a. Theory and simulation of stochastically-gated diffusion-influenced reactions. *J. Phys. Chem.* 100:2597–2604.

Zhou, H.-X., and A. Szabo. 1996b. Theory and simulation of the time-dependent rate coefficients of diffusion-influenced reactions. *Biophys. J.* 71:2440–2457.